Morphology And Mechanical Behavior of Commercially Available Caco₃ And Organically Modified Caco₃ Filled Natural Rubber Composite Vulcanizates

*Dr. Mausumi Saha
Department of Chemistry, Raja Peary Mohan College
*Corresponding Author: *Dr. Mausumi Saha*

ABSTRACT: Commercially available and organically modified calcium carbonate-natural rubber (NR) composites have been prepared through Brabender mixture. All the composites were found to have higher modulus and tensile strength than the gum vulcanizates. Modified filler-composite was found to have increased modulus over a certain (200%) deformation with respect to unmodified filler composite. The effect of different weight percentages of calcium carbonate loading in NR composites was studied. The term 'E-inequality' means Mooney-Rivlin material model assumes that $C_1 > 0$ and $C_2 \leq 0$. Present investigation shows that the above assumption should be relaxed for the behavior of calcium carbonate–NR composite under tension. The stress-strain behavior at low, moderate and high strains is not identical. Therefore, different mechanisms need to be implemented for the rubber vulcanizates at different strain modes. According to molecular concept, this behavior is attributed to strain-induced changes in network topology (such as entanglements). Morphology study reveals that morphology change may take place during mixing and compression molding. The untreated CaCO3 particles adsorb NR chain to form sandbag of CaCO3 embedded in NR by mechanical shear forces and highly dispersed structured of PMMA modified $CaCO_3$ in composites.

Keywords: Mooney-Rivlin material model, Tensile properties, PMMA encapsulation, Calcium carbonate, Polymerization

I.   INTRODUCTION

Component like filler in the recipe of elastomeric compound is of great interest as it forms a large family of desirable materials. Behavior of filler depends on many factors as size, aspect ratio, agglomeration affinity and dispersion – distribution ability in the elastomeric matrix. Modification of the filler particles changes almost all the above characteristics in comparison to the virgin one. The elastic behavior of vulcanized rubber may be taken as a quantitative basis for evaluating the effect of filler on stiffness and strength[1]. The methodology for the analysis of elastic behavior is two fold: (i) statistical or kinetic theory from some idealized theoretical models of elastomer's structure, and (ii) the phonological theory from the perspective of continuum mechanics[2]. The methodology as if modified Mooney-Rivlin material model equation for the mechanical behavior analysis of rubber-like materials in finite elasticity may be proposed to describe the behavior of material nonlinearities[3]. In the present study, the comparisons between whiting (calcium carbonate) and poly (methyl methacrylate) (PMMA, oligomer) modified whiting have been investigated in terms of filler loading and oligomer modification. A scanning electron micrograph (SEM) morphology study reveals the fracture surface of both types of filler vulcanizates.

II.   EXPERIMENTAL

2.1 Encapsulation of whiting (CaCO₃) with PMMA oligomer:
The encapsulation of whiting (CaCO₃) with PMMA oligomer was done using dispersion polymerization process[4,5].

Materials
Whiting, in the form of fine powder, was provided by Chemical and Mineral Industries Pvt. Ltd., Rajasthan, India. Its specification was: specific gravity 2.60, bulk density (gm/ml) 1.10, D.O.P absorption (g/100g) 25, moisture content 0.07, silica (SiO₂) 0.02, iron oxide (Fe₂O₃) 0.01, alumina (Al₂O₃) 0.05, calcium carbonate (CaCO₃) 98.5, fineness 99.9% (through B.S. sieve 410 mesh). Reagent grade chemicals were used as such. Methyl methacrylate, ammonium persulfate and toluene (all A.R. grades) were procured from standard sources. Sodium salt of polyacrylic acid (Aldrich) was used as dispersing agent.

2.2 Filler-Rubber composite preparation
Raw Materials

The natural rubber (Mooney viscosity, ML_{1+4} 72 at 100°) was obtained from Kerala Rubber Board, India. Zinc oxide (99%), stearic acid, BSM, IPPD and sulfur were procured from local market. Raw whiting (commercial) and modified whiting were used. The formulation of the rubber composites and their designation are shown in Table 1.

Methods

All mixes were prepared using a Brabender machine (Plastograph Electronical Torque Rheometer type 815606, Germany) according to ASTM D-3192, working at 70^0 with a rotor speed of 60 rpm, 5 min for cold mastication, and another 15 min for mixing of the ingredients except sulfur. Finally, sulfur was mixed on a laboratory size two-roll mill (30 cm x 15cm) following ASTM D-3185-88. The compound was taken out in sheet form and tested with a Monsanto ODR 100 instrument to obtain optimum cure time at curing temperature of 150^0 with a micro die and 3^0 arc of oscillation. Cross-linking or curing of the compounded samples was carried out in hot press at 150^0.

2.3 Testing and Characterization
Tensile Test

Tensile stress-stain properties were carried out according to ISO-37 using dumb-bell specimens at 25 ± 2^0. Test samples were punched from the vulcanized sheets parallel to the grain directions using a dumb-bell die (9C-type). Thickness of the sample was measured by bench thickness gauge. Samples were tested in an Universal testing machine (UTM LR 10K PLUS, LLOYD Instrument Ltd., Hemetek Techno Instrument, Inc.) at a crosshead speed of 50 cm/min. Modulus (load at 300 % elongation) was recorded and elongation at break was measured.

Swelling characteristics and crosslink density measurement

For each vulcanized sheets, the value of M_c (mean chain segment molecular weight) was calculated by measuring equilibrium-swelling volume in benzene and with the help of quantitative expression of the Flory – Rehner equation[6],

$$\rho\, V_s\, V_r^{\frac{1}{3}} / M_c = - [\, \ln (1- V_r) + V_r + \chi\, V_r^2\,] \qquad (1)$$

where ρ, density of rubber; V_s, molar volume of solvent; V_r, volume fraction of rubber in swollen gel; χ, interaction parameter for rubber- solvent system. $1 / M_c$ is the crosslink density of the vulcanizate.

Scanning electron microscopy

The phase morphology of $CaCO_3$ –filled NR composites was studied through scanning electron microscopy (SEM). The examination was performed with a Scanning electron microscope S3400N (Hitachi, Japan) at 15 and 5 kV, and the specimens were coated with a thin layer of gold before SEM examination.

III. RESULTS AND DISCUSSION

3.1 Stress- strain curve

Formulations of the composite mixes are given in Table 1. Sample S_0 (gum), two raw (untreated) filler loaded rubber composite samples and three treated (PMMA coated) filler loaded rubber composite samples were cured at 150^0. Stress-strain graphs for composites (Figure 1) reveal that slope of the initial portion increases with filler loading. In addition, the slope of the ending portion of gum (S_0 vulcanizate) is highest in comparison. This is for easy chain alignment possibility in the gum vulcanizate by orientation of the network structure in the direction of stretching by the applied force. Initial and ending portions of each graph indicate modulus and ultimate tensile strength respectively.

3.2 Tensile strength properties

The data for variation of tensile strength properties (modulus, elongation and others) for gum and the various composites are given in Table 2. The tensile properties of various composites are plotted against the weight percentage of $CaCO_3$ content (ignoring very small PMMA amount) in Figure 2 for better understanding of the effect of treated and untreated filler in the mix. The results for gum compound have shown in Figure 2 for comparison. The percentage variations of various properties have been furnished in Table 3. It can be seen that the tensile strength is improved with increasing CaCO3 filler incorporation. The results showed that the modified CaCO3filled composite, S_3 (10 phr coated filler loaded), can strengthen NR composite. The reason should be that CaCO3 particles (coated with polymer) can be well distributed in matrix. The T.S. value increases from 4.3 MPa to 5.04 MPa (at 10 phr coated filler loaded composite, S_3). This may be the results of surface treatment (encapsulation) of filler tends to meet the law of minimum total free energy (the values of surface tension of $CaCO_3$ at 25^0 C and $CaCO_3$-PMA at 25^0C are 158.3 and 47.1 mJ/ m^2 respectively. After

surface modification, the surface tension (γ) of CaCO₃ particles is markedly decreased, which means the surface free energy of CaCO₃ are greatly decreased. This trends to decrease aggregation of CaCO₃ particles to improve dispersion of CaCO₃ particles in the polymer and compatibility between CaCO₃ particles and polymer).

When more than 10phr modified-CaCO3 fillers are filled, encapsulated fillers are close enough, they form aggregates and creates difficulty in uniform dispersity. It induces a local stress concentration inside the composites. As a result, the rubber composite containing higher amounts of modified-CaCO3 deform in a brittle manner and have relatively lower tensile strength during tensile deformation. Generally, elongations at break have been found to diminish with loading of filler. In the present work, PMMA coated CaCO₃–loaded composites show comparable trend except S_3 (the elongation at break of 10phr modified-CaCO3 filler increases from 691% to 772%, which indicates that 10phr modified-CaCO3 filler particles can toughen the composite). Adequate dispersion of filler particles lubricated by the PMMA oligomer, increases stress concentration center remarkably to improve the elongation at break of S_3. But the critical concentration of the modified filler is about 10phr, when the highest elongation at break was achieved. The function of PMMA in the coated structure seems to be limited if the PMMA/ CaCO3 adhesion is not strong enough. Another interesting phenomenon lies in that the surface modification of CaCO3 also has a pronounced influence on the modulus values of the composites. The results show higher modulus values for both types of filler composites. Because the affinity of CaCO3 towards the rubber matrix is high, moreover by treating CaCO3 with PMMA, there are energetically elastic CaCO3 network within the NR matrix, The percentage of different types of cross-linking bonds in coated filler composites may be the cause for initial increase in modulus[7,8].

3.3 Analysis of deformation characteristics at various extensions

For further understanding of filler characteristics, modulus values at various extensions have been analyzed. In this attempt to compare the PMMA coating influence, the ratio R_f of vulcanizate modulus is used. Here, R_f is the ratio of modulus at given elongations of the filled vulcanizate to that of unfilled (gum) vulcanizate. R_f value is plotted as a volume fraction of filler[9] and shown in Figure 3. It is clear that the R_f value of 40 phr CaCO₃ loaded composite (S_2) increases drastically. This increase seems to be related to filler-filler and filler rubber interactions[10]. The mechanism involved should be studied further. At least, an elastomer encapsulation with high affinity to the CaCO₃ particles inclusions would favor the absorption of energy.

The identification of the effect of filler modification on strength properties is very difficult because rubber is cross-linked in a random manner. For lightly reinforced filler-rubber composite, Smallwood's theoretical expression[11] relating to elastic modulus is shown in equation (2). For high concentration of reinforcing filler, Kontou and Spathis[12] proposed a theoretical expression as equation (3).

$M_f = M_0 (1+2.5\varphi)$ (2)

Modified equation, $M_f = M_0 (1+2.5\varphi +14.1\varphi^2)$

$M_f = M_0 (1+0.67f\varphi +1.62f^2 \varphi^2)$ (3)

where M_f, M_0 are modulus of filled and unfilled vulcanizates respectively, and Φ, f are volume concentration and shape factor of the filler respectively.

Fitting of the experimental values to these equations is very difficult and ambiguous for various reasons. Therefore, Mooney-Rivlin material model has been adopted.

3.4 Mooney-Rivlin material model

The non-equilibrium stress-strain data are fitted to the Mooney-Rivlin-Saunders equation[13]. It is a hyper elastic material model, also called polynomial hyper elastic model[14].

The equation:

$$F[A_0 ((\lambda-\lambda^{-2})]^{-1} = 2C_1 + 2 C_2 \lambda^{-1}$$ (4)

where F is the force required to stretch a vulcanizate sample of unstrained cross-sectional area A_0 at an elongation ratio λ and λ is defined as $1 + \varepsilon$, where ε is the strain produced by stress σ. C_1 is a constant pertaining to ideal elastic behavior. It is related to number average molecular weight of rubber before cross-linking ($\overline{M}_n$) and average molecular weights between cross-links ($\overline{M}_c$). The term C_2 is a constant, which indicates departures from ideal elastic behavior. At sufficiently high degree of swelling of vulcanizate, C_2 will be zero. Therefore, it is accepted that C_1 is a perfect network parameter but C_2 gives indication about achievement of equilibrium. The Mooney-Rivlin equation can be viewed as an extension of the neo-Hookean form. It includes a term that depends on the second invariant of the left Cauchy-Green tensor. In many cases, it will provide a more perfect in shape to the investigational information than the neo- Hookean mode. The above expression is a linear form like, y = mx + b, where m is the slope indicating second Mooney-Rivlin constant C_2, and b the intercept, giving first Mooney-Rivlin constant C_1.

In the present investigation, we looked at the procedure for determining the Mooney-Rivlin constants from simple tensile test data of $CaCO_3$ filled NR vulcanizates at three (low, moderate and high) deformations. All the experimental stress-strain curves, $(F/A_0) / (\lambda - \lambda^{-2})$ versus $1/\lambda$, are shown in Figures 4-5. We used Origin 6.0 professional software for this plot. It is clear from Figure 4 that all the curves show significant upturn at higher elongations, i.e. with the increase of $1/\lambda$ (high to low elongation), the ordinate values decrease initially, reaching a minimum, and increasing finally. It is clear that Mooney-Rivlin is not valid for all range of strains. The deviations are clearly noticeable if stress-strain nature is compared for different modes of deformation. In Table 4, values of Mooney parameters $2C_1$ and $2C_2$ of the $CaCO_3$-NR composites are presented. Gum vulcanizate (S_0) is evaluated for comparison. It is generally accepted that $C_1 > 0$ and $C_2 \leq 0$, which is known as E-inequalities. It is established on the postulation of the free energy function, which is positive for any deformation. The experimental facts for rubber-like substances are in line with the above[15-17]. The results of C_1 and C_2 (Table 4) show that the behavior of S_0 and S_5 composites at low (0-120% strain) and moderate (121-400% strain) stretch ratios and S_0, S_1, S_4 and S_5 composites at high (>400% strain) stretch ratio, perfectly support the general postulation. The other results where C_1 values are negative and C_2 values are positive are not agreeable with the general postulation. Liu showed that C_2 need not be negative for isothermal uniaxial compressive stress-strain experiment (curves are increasing and concave upward)[15]. The reason is the locking behavior (the material turns harder and harder to contact as the compressive strain increases) under confined compression. According to Liu's thermodynamic stability analysis, it follows that

$$\frac{C_2}{C_1} \leq \frac{1}{3}(2\lambda + \lambda^4) \qquad (5)$$

Clearly, this is a limit for possible values of the parameters C_1 and C_2. Especially, for $\lambda = 1$, the above expression gives $C_1 \geq C_2$. It means that this condition is always fulfilled for uniaxial extension, $\lambda > 1$. However, no such results were observed in the literature, which supports these experimental findings under uniaxial tension. Therefore, it seems that the results (S_0, S_1, S_4 and S_5 composites at high (>400% strain) stretch ratio, Table 4) do not satisfy the E-inequalities in Mooney-Rivlin model, even though Liu concluded "it is not necessary to require that the material parameter C_2 be negative as proposed by the E-inequalities, but rather only $C_2 < C_1$". The most of the C_2 values in the Table 4 should remain a subject of debate tomorrow[18]. Yet it is an independent parameter associated with a failure to achieve equilibrium in swelling. At moderate strain, there is a trend that the constant C_1 increases with increasing filler loading. As C_1 value indicates the number of network chains per unit volume (crosslink density) according to rubber elasticity theories, moderate and high strain data suggest homogeneous composites formed in all the PMMA coated $CaCO_3$ filled NR vulcanizates.

To investigate the validity of Mooney-Rivlin model for the present experimental data of S_0 and S_5 vulcanizates at various strains (different C_1 values), a plot of σ/C_1 versus ε is shown in Figure 6. The decreasing behavior in this uniaxial tension experiment clearly indicates that the model is valid up to 400% strain for S_0 but for almost all strain for S_5. The result (for S_5, Table 4) is interesting technologically. In these results C_2/C_1 is negative i.e. < 0. Other ratios of C_2/C_1 presented in the Table 4 give no clear indication about the attachment between NR and $CaCO_3$ particles and the interface formation, if any, to the composite network structure.

3.5 Interpretation of stress-strain behavior of the $CaCO_3$ filled NR Vulcanizates samples according to molecular concept

The prime assumption in this concept is that the molecular chains obey Gaussian statistics. It is then established that the free energy of deformation per unit volume of rubber (strain energy density, W) is in the form

$$W = \frac{1}{2}NkT(\lambda_1^2 + \lambda_2^2 + \lambda_3^2 - 3) \qquad (6)$$

where N, k, T and ($\lambda_1, \lambda_2, \lambda_3$) are crosslink density (number of net work chains per unit volume), Boltzmann's constant, absolute temperature and principle extension (stretch) ratios respectively. For simple extension, $\lambda_1 = \lambda$ and $\lambda_2 = \lambda_3 = \lambda^{-1/2}$ and the empirical relation from kinetic theory of rubber-like elasticity is,

$W = \frac{1}{2} NkT [\lambda^2 + 2(\lambda^{-1/2})^2 - 3]$

$W = 1/2 NkT(\lambda^2 + 2\lambda^{-1} - 3) \qquad (7)$

Therefore, stress-strain relation will be

$$\frac{\partial W}{\partial \lambda} = \sigma = NkT(\lambda - \lambda^{-2}) \qquad (8)$$

where σ is the normal tensile strength. Hence, $[\sigma / (\lambda - \lambda^{-2})]$ should be constant. However, in practice, it is not constant; it falls as λ increases. For simple extensions, the load deformation relation can be expressed for a homogeneous, isotropic and incompressible elastic sample. The relation is

$$W = C_{10}(I_1 - 3) + C_{01}(I_2 - 3) \qquad (9)$$

where I_1 and I_2 are the two functions of strain invariants of the Green deformation tensor, viz.
$I_1 = \lambda_1{}^2 + \lambda_2{}^2 + \lambda_3{}^2$ and $I_2 = \lambda_1{}^2 \lambda_2{}^2 + \lambda_2{}^2 \lambda_3{}^2 + \lambda_3{}^2 \lambda_1{}^2$
In simple extension, the values are
$I_1 = \lambda^2 + 2/\lambda$ and $I_2 = 1/\lambda^2 + 2\lambda$

By differentiation of the stress-strain relations (Equation 9) involving partial derivatives, the relation is

$$\sigma = \frac{F}{A_0} = \frac{\partial W}{\partial \lambda} = 2\left[\frac{\partial W}{\partial I_1} + \frac{\partial W}{\partial I_2}\lambda^{-1}\right](\lambda - \lambda^{-2}) \qquad (10)$$

where F is the force to produce the simple extension ratio λ.
Again, A_0 = thickness (h) x width (B). So

$$F/B = 2h\,(\lambda - \lambda^{-2})\left[\frac{\partial W}{\partial I_1} + \frac{\partial W}{\partial I_2}\lambda^{-1}\right]$$

$$\text{Or, } L/2h\,(\lambda - \lambda^{-2}) = \frac{\partial W}{\partial I_1} + \frac{\partial W}{\partial I_2}\lambda^{-1} \qquad (11)$$

where L is the load per unit width. By plotting $L/2h\,(\lambda - \lambda^{-2})$ versus λ^{-1}, the dependence of

$[\frac{\partial W}{\partial I_1} + \frac{\partial W}{\partial I_2}\lambda^{-1}]$ on $1/\lambda$ could be understood.

The values of $L/2h\,(\lambda - \lambda^{-2})$ and λ^{-1} were calculated for CaCO$_3$–NR composite vulcanizates and the results are shown in Figure 7. The plots show that the general trend in each case of each composite is same. The plots indicate that the value of $\left[\frac{\partial W}{\partial I_1} + \frac{\partial W}{\partial I_2}\lambda^{-1}\right]$ reaches a minimum in each of the CaCO$_3$-NR composites.

With increase of $1/\lambda$ (1/ elongation ratio), the value of $\left[\frac{\partial W}{\partial I_1} + \frac{\partial W}{\partial I_2}\lambda^{-1}\right]$ increases after the minimum.

However, the modulus value of the composite increases with the increase of $\left[\frac{\partial W}{\partial I_1} + \frac{\partial W}{\partial I_2}\lambda^{-1}\right]$. This

relationship may be due to the linearity of the curve and reversibility of the composite vulcanizates and may arise from the Gaussian character of the chains.

It may be concluded that though the molecular concept elucidates the key characteristics of rubber elasticity, unluckily the concept is not applicable for all range of deformations. Deviations at moderate strains are explained by the theory of contribution to the energy stored in the molecular chain during stretching. Energy stored decreases as the chain is stretched[2] and the deviations in large strains are explained by strain-induced crystallization. The explanation above is definitely suitable for Gaussian statistics but for non-Gaussian statistics, it is very difficult to conclude anything due to complexity of mathematics. Therefore, the attempt for the validity of the Mooney-Rivlin model is partially successful quantitatively with the present experimental data.

3.6 Morphological analysis
SEM micrographs with 1000 times magnification of the tensile fracture surfaces of NR vulcanizates filled with different amounts of unmodified CaCO3, modified nano-CaCO3 are shown in Fig.8 (c-h). Figures 8 (a,b) show the SEM photographs of unmodified and modified CaCO$_3$ respectively. It is interesting to observed very distinct features in the two cases. The unmodified CaCO$_3$ shows irregular shape. Modified particle is round shaped. This is for PMMA very smooth surface embedded with some small particles. These particles are likely to be zinc oxide (ZnO). The smoothness indicates no mechanically weaker region for crack initiation. When unmodified CaCO3 was filled in NR matrix, The morphology change may take place during mixing. The CaCO3 particles adsorb NR chain to form sandbag of CaCO3 embedded in NR by mechanical shear forces. This sandbag of CaCO3 embedded in NR is called filler network or cluster (Fig.8d-e). This filler network may be the cause of improved physical properties of 20 and 40 phr unmodified CaCO$_3$ composites (S$_1$ and S$_2$). Generally, as the number of unmodified filler particles increases the filler particles form agglomeration in rubber matrix. In this experiment, a few not many agglomerations are found in SEM micrographs of S$_1$ and S$_2$ to be investigated, rather the formation of a shell around the filler is partially noticed. This may be the results of high affinity of NR to CaCO$_3$ particles.

Highly dispersed structured of composite vulcanizates was observed in SEM figures of PMMA modified CaCO$_3$ composites (Figures 8-f to h for S$_3$, S$_4$ and S$_5$ respectively). CaCO$_3$ as the island phase well distributed in NR as the sea phase. However, modified composites gave optimum strength properties up to 10

phr filler loading and dropped when loading was more. The reduction in modulus at higher loading was dependent on degree of dispersion and agglomeration of fillers, but the mechanism is not clear from SEM pictures (Figures 8 - f to h).

Concluding remarks

In the present study, PMMA modified calcium carbonate-filled NR vulcanizate at lower filler loading (10 phr) has shown better modulus and rubber-filler interaction compared to unmodified calcium carbonate-filled NR vulcanizates. One important feature that emerges from the present study is that the Mooney-Rivlin model is valid for gum and PMMA modified filler composite (20 phr filler loading, S_5), but it fails to support the behavior of other filler loaded composite vulcanizates. The results reveal that the PMMA modified $CaCO_3$-NR composites demonstrate well dispersion, less agglomeration and significant wettability of the filler in the rubber matrix, which is attributed to better modulus and other properties. Thus, it may be concluded that polymer modification of the filler enhances higher degree of dispersion in NR matrix.

References

[1]. Sobby, M.S. Elastic behavior of ternary rubber-filled vulcanizates, Polym. International **1997**, 42, 85-89.

[2]. Yeoh, O.H. ; Fleming, P.D. A new attempt to reconcile the statistical and Phenomenologyical theories of rubber elasticity, J. Polym. Sci. Part B: Polym. Phy. **1997**, 35,1919-1931.

[3]. Meissner, B.; Matějka, L. Description of the tensile stress-strain behavior of filler-reinforced rubber-like networks using a Langevin-theory-based approach. Part I, Polymer **2000**, 41, 7749-7760.

[4]. Bourgeat-Lami, E.; Lang, J.J. Encapsulation of inorganic particles by dispersion polymerization in polar media, J. Coll. Interface Sci. **1998,** 197, 293-308.

[5]. Konar, B.B.; Saha, M. Influence of polymer coated $CaCO_3$ on vulcanization kinetics of natural rubber/sulfur/N-oxydiethyl benzthiazyl sulfonamide (BSM) system, J. Macromol. Sci. Part A: Pure and Applied Chem. **2012,** 49, 214-226.

[6]. Morrel, S.H. Rubber Technology and Manufacture, 2ⁿᵈ Ed.,Blow C. M, Hepburn C. Eds. Butterworths, London, **1987**, p.189.

[7]. Ibarra, L.; Alzorria, M. Ionic Elastomers Based on Carboxylated Nitrile Rubber(XNBR) and Zinc Peroxide: Influence of Carboxylic Group Content on Properties, Polym. Int. **1999,** 48, 580-

[8]. 592.

[9]. Ibarra, L.; Alzorria, M. Ionic Elastomers Based on Carboxylated Nitrile Rubber (XNBR) and Zinc Peroxide: Influence of Carboxylic Group Content on Properties, J. Appl. Polym. Sci. **2002,**

[10]. 84, 605-615.

[11]. Chae , H.D.; Basuli, U.; Lee, J.H.; Lim, C.I.I.; Lee, R.H.; Kim, S.C.; Jeon, N.D.; Nah, C. Mechanical and Thermal properties of rubber composites reinforced by zinc methacrylate and carbon black, Polym. Composites **2012,** 1141-1153.

[12]. Eggers, H.; Schummer, P. Reinforcement mechanisms in carbon black and silica loaded rubber melts at low stresses, Rubber. Chem. Technol. **1996,** 69, 253-261.

[13]. Payne, A.R., Reinforcement of Elastomers, ed. G. Kraus, Wiley Interscience, New York,**1965**, p 76.

[14]. Kontou, E.; Spathis, G. Elastic behavior of natural rubber filled vulcanizates J. Appl. Polym. Sci. **1990,** 39, 649-662.

[15]. Mark, J.E.; Earman, B. Rubberlike Elasticity, A Molecular primer, Wiley-Interscience, New York, **1989**.

[16]. [14] Bower, A. Applied Mechanics of solids, CRC Press, ISBN[[SpecialBooksources/1- 4398-0247-2 l1- 4398-0247-2]] January 2010. Liu, I-Shih. A note on the Mooney-Rivlin material model, Instituto de Matemática, Universidade Federal do Rio de Janeiro 21945, Rio de Janeiro, Brasil, Springer **2008.**

[17]. Müller I. Rubber and Rubber Balloons, Springer **2004**.

[18]. Truesdell, C.; Noll, W. The Non-Linear Field Theories of Mechanics, Third Edition, Springer **2004**.

[19]. [18] Wagner, M.H. The origin of the C2 term in rubber elasticity, J. Rheol. **1994,** 38, 655-679.

Table 1. Composition of rubber chips in six different formulas **(Basic recipe of the mix samples)**

Ingredient	S_0	S_1	S_2	S_3	S_4	S_5
Natural rubber (RMA- IX)	100.0	100.0	100.0	100.0	100.0	100.0
Zinc oxide	4.5	4.5	4.5	4.5	4.5	4.5
Stearic acid	1.5	1.5	1.5	1.5	1.5	1.5

IPPD[a]	1.0	1.0	1.0	1.0	1.0	1.0
Sulfur	2.0	2.0	2.0	2.0	2.0	2.0
BSM[b]	2.0	2.0	2.0	2.0	2.0	2.0
Whiting[c] (unmodified, CC)	-	20.0	40.0	-	-	-
Whiting[d] (modified, PCC)	-	-	-	10.0	15.0	20.0
CaCO3 weight %	0	13.76	23.87	7.45	10.73	13.76
Volume fraction Of CaCO3	0	0.0643	0.1213	0.0333	0.0493	0.0643

a…Isopropyl paraphenylene diamine
b…N-Oxydiethyl benzthiazyl sulfenamide
c…Natural calcium carbonate (CC)
d…PMMA coated whiting (PCC)

Table 2 Sample test specification: Direction: Tension; speed: 500 mm/min; Gauge length 25 mm; Width 4.45 mm; Thickness 1.80 mm; Area 8.01 mm^2

Properties	S_0	S_1	S_2	S_3	S_4	S_5
Tensile strength (MPa)	4.3	4.35	5.09	5.04	4.52	4.50
Elongation at break (%)	691	689	579	772	652	633
Elongation at fracture (mm)	172	184	144	193	163	158
Stiffness (N/m)	985	284	608	530	600	1210
Modulus at :						
25% elongation (MPa)	0.05	1.25	1.21	0.72	0.75	0.76
50% elongation (MPa)	0.12	1.35	1.61	1.09	0.92	0.90
100% elongation (MPa)	0.33	1.53	2.07	1.38	1.25	1.17
200% elongation (MPa)	0.74	1.88	2.69	1.91	1.76	1.63
300% elongation (MPa)	1.16	2.23	3.31	2.46	2.25	2.14
400% elongation (MPa)	1.57	2.58	3.93	3.00	2.69	2.60
500% elongation (MPa)	2.64	2.94	4.55	3.55	3.28	3.08

Table3 Tensile properties (change in Percentage) of the composites over gum compound vulcanizate

	Coated filler rubber composite			Uncoated filler rubber composite	
	S_3	S_4	S_5	S_1	S_2
Tensile strength change%	17.21	5.11	4.65	1.16	18.37
Elongation at break change%	+11	-5	-8	-0.2	-16
Change % :					
Modulus at 25% elongation	+1340	+1400	+1420	+2400	+2320
Modulus at 50% elongation	+808	+666	+650	+1025	+1241
Modulus at100% elongation	+318	+278	+254	+363	+527
Modulus at 200% elongation	+158	+137	+120	+154	+263
Modulus at 300% elongation	+112	+93	+84	+92	+185
Modulus at 400% elongation	+91	+71	+65	+64	+150
Modulus at 500% elongation	+34	+24	+16	+11	+72

Table 4: **Values of Mooney-Rivlin constants(C_1 and C_2)obtained from stress-strain curves at low-middle, high, very high strain.**

| Sample	At low strain (0 to120%)			at high strain (121 to 400%)			at very high strain (>401%)		
	$2C_1$ (MPa)	$2C_2$ (MPa)	C_2/C_1	$2C_1$ (MPa)	$2C_2$ (MPa)	C_2/C_1	$2C_1$ (MPa)	$2C_2$ (MPa)	C_2/C_1
S_0	0.41699	-0.45328	-1.08	0.45985	-0.60771	-1.32	1.10677	-3.95428	-3.57
S_1	-2.04554	5.14080	-2.51	0.30924	1.04302	3.37	0.64599	-0.92196	-1.42
S_2	-1.57790	5.08858	-3.22	0.55935	1.13402	2.02	0.63734	0.75385	1.10
S_3	-0.19776	1.91788	- 9.69	0.51099	0.46100	0.50	0.54323	0.31499	0.58
S_4	0.05856	1.23194	21.03	0.45103	0.48230	1.07	0.70346	-0.88901	-1.26
S_5	0.84346	-0.54462	-0.64	0.96981	-0.82831	-0.85	0.99346	-0.93680	-0.94

Caption of Figures

Figure 1.   Stress-strain plot of coated and uncoated composite vulcanizates.
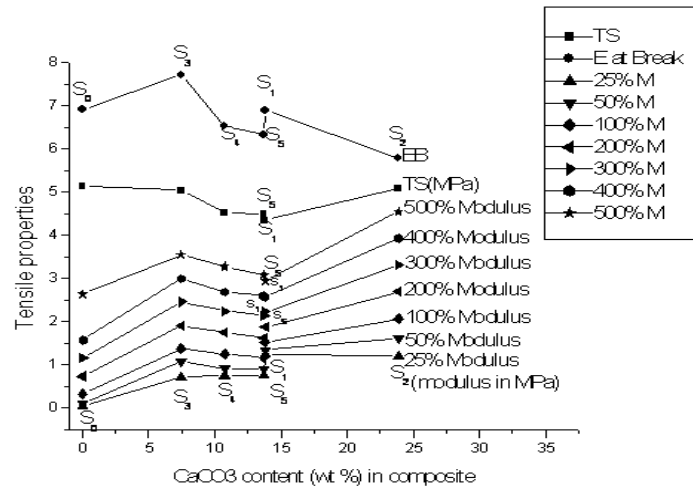
Figure 2.   Tensile Properties of gum (S_0), untreated filler loaded composites (S_1 and S_2) and PMMA coated filler composites (S_3, S4 and S_5).
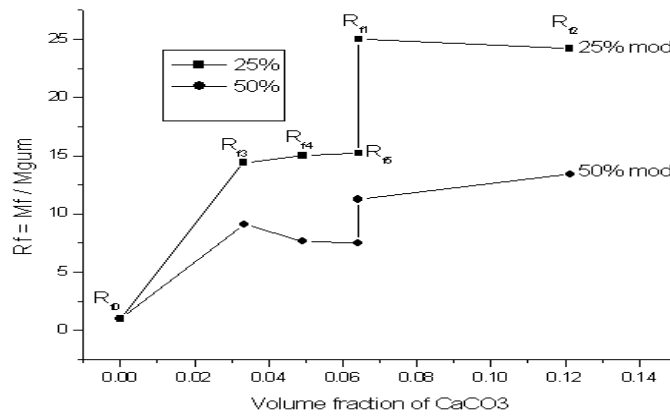
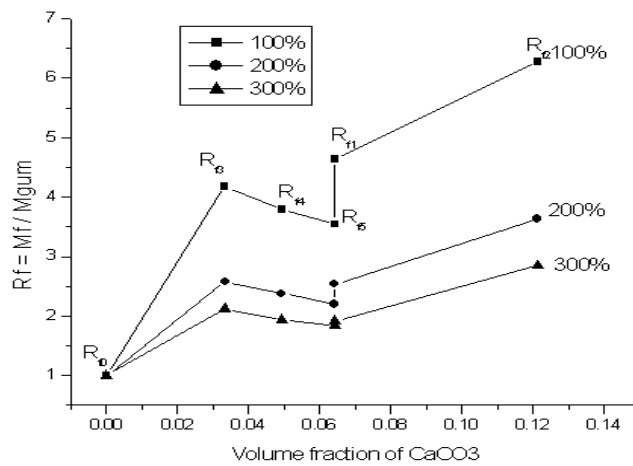Figure 3.   a. Increase in modulus, as a volume fraction of $CaCO_3$ expressed as ratio R_f at low Strain b. Increase in modulus, as a volume fraction of $CaCO_3$ expres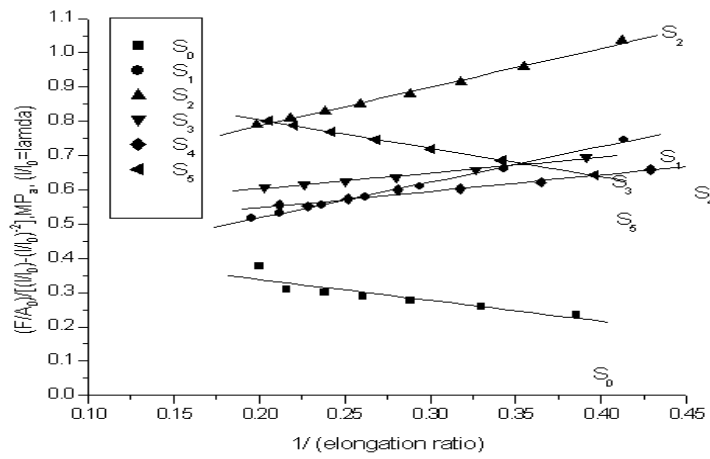sed as ratio R_f at moderate Strain c. Increase in modulus, as a volume fraction of $CaCO_3$ expressed as ratio R_f at high Strain

Figure 4. $[(F/A_0) / (\lambda - \lambda^{-2})]$ versus $1/\lambda$ plots of all $CaCO_3$ filled NR vulcanizate samples.

Figure 5. a. Mooney – Rivlin plot of $CaCO_3$ filled NR vulcanizates samples at low elongations

b. Mooney – Rivlin plot of $CaCO_3$ filled NR vulcanizates samples at moderate elongations

c. Mooney – Rivlin plot of $CaCO_3$ filled NR vulcanizates samples at high elongations

Figure 6. σ/C_1 versus ε plot for S0 vulcanizate at various strain having different C_1 values.

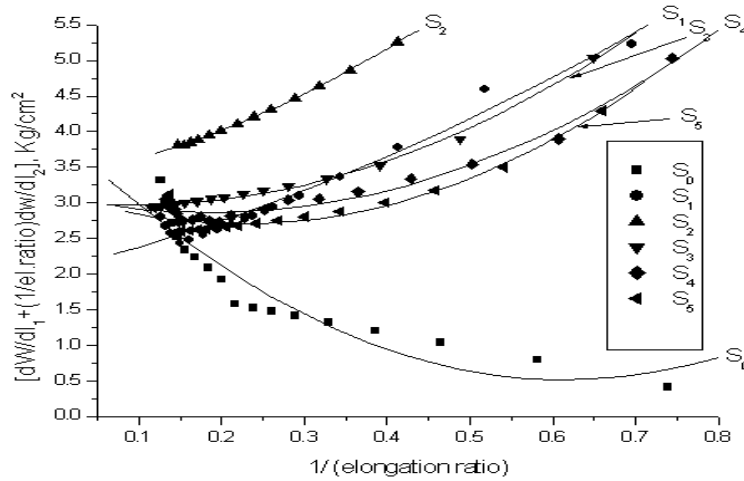Figure 7. Plots of $\left[\dfrac{\partial w}{\partial I_1} + \dfrac{\partial w}{\partial I_2} \right]$ vs $1/\lambda$ for $CaCO_3$ –NR composite vulcanizates on simple extension.
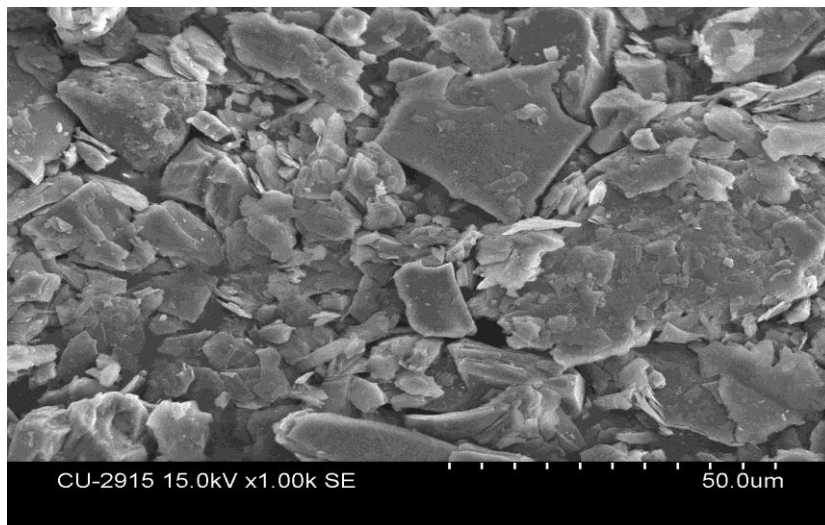
Figure 8.   a. SEM observation of the surface of $CaCO_3$ and NR/$CaCO_3$ composite for unmodified $CaCO_3$ (1000X)

8b. SEM observation of the surface of $CaCO_3$ and NR/$CaCO_3$ composite for PMMA modified $CaCO_3$ (1000X)

8c. SEM observation of the surface of $CaCO_3$ and NR/$CaCO_3$ composite for gum compound(S_0) (5000X)

8d. SEM observation of the surface of $CaCO_3$ and NR/$CaCO_3$ composite for 20 phr $CaCO_3$/NR composite (S_1) (1000X)

8e. SEM observation of the surface of $CaCO_3$ and NR/$CaCO_3$ composite for 40 phr $CaCO_3$/NR composite (S_2) (1000X)

8f. SEM observation of the surface of $CaCO_3$ and NR/$CaCO_3$ composite for 10 phr modified $CaCO_3$/NR composite (S_3) (1000X)

8g. SEM observation of the surface of $CaCO_3$ and NR/$CaCO_3$ composite for 15 phr modified $CaCO_3$/NR composite (S_4) (1000X)

8h. SEM observation of the surface of $CaCO_3$ and NR/$CaCO_3$ composite for 20 phr modified $CaCO_3$/NR composite (S_5) (1000X)
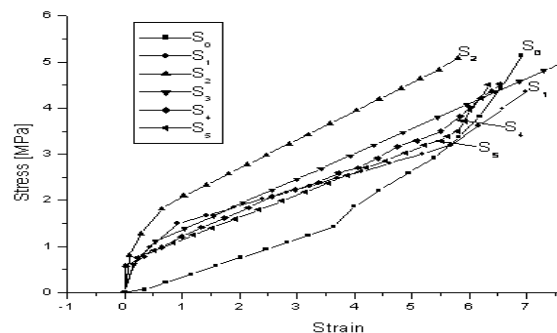
Figure 1 Stress-strain plot of coated and uncoated composite vulcanizates.

Figure 2. Tensile Properties of gum (S$_0$), untreated filler loaded composites (S$_1$ and S$_2$) and PMMA coated filler composites (S$_3$,S$_4$ and S$_5$).

Figure 3a. Increase in modulus, as a volume fraction of CaCo$_3$ expressed as ratio R$_f$ at low Strain

Figure 3b. Increase in modulus, as a volume fraction of CaCo$_3$ expressed as ratio R$_f$ at moderate Strain

Figure 3c. Increase in modulus, as a volume fraction of CaCo$_3$ expressed as ratio R$_f$ at high Strain

Figure 4. [(F/A$_0$) / ($\lambda - \lambda^{-2}$)] versus 1/λ plots of all CaCO$_3$ filled NR vulcanizates

Figure 5a. Mooney – Rivlin plot of CaCO$_3$ filled NR vulcanizates samples at low elongations

Figure 5b. Mooney – Rivlin plot of $CaCO_3$ filled NR vulcanizates samples at moderate elongations
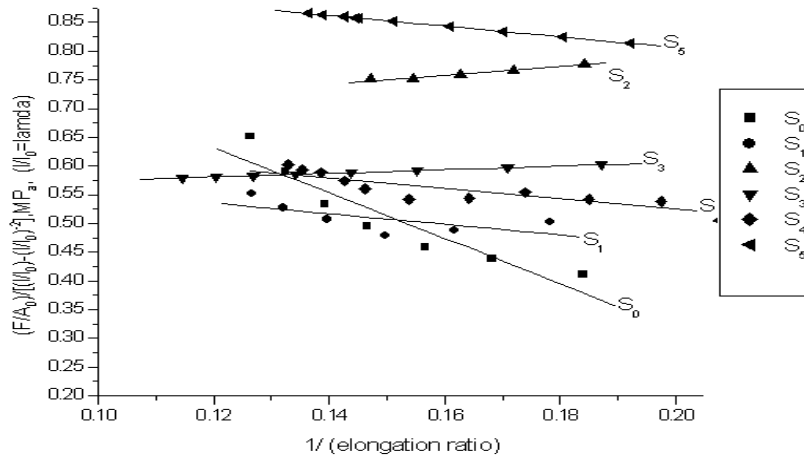
Figure 5c. Mooney – Rivlin plot of $CaCO_3$ filled NR vulcanizates samples at high elongations
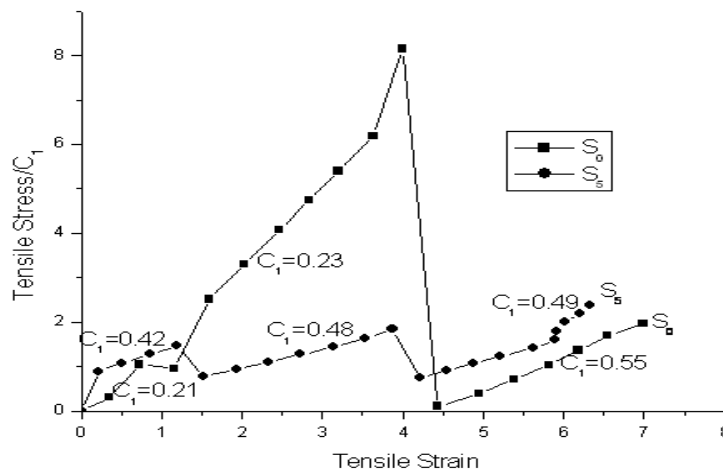
Figure 6. σ/C_1 versus ε plot for S0 vulcanizate at various strain having different C_1 values

Figure 7. Plots of $\left[\dfrac{\partial w}{\partial I_1} + \dfrac{\partial w}{\partial I_2}\, \lambda^{-1}\right]$ vs $1/\lambda$ for $CaCO_3$ –NR composite vulcanizates on simple extension.

Figure 8a. SEM observation of the surface of $CaCO_3$ and NR/$CaCO_3$ composite for unmodified $CaCO_3$ (1000X)
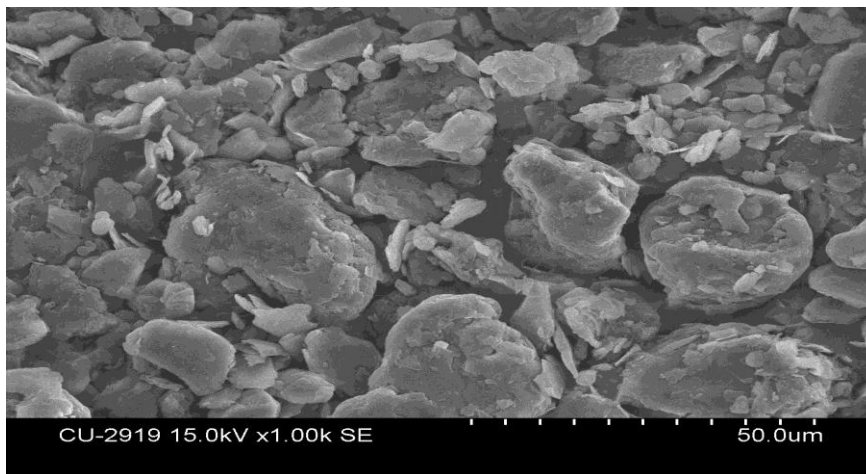
Figure 8b. SEM observation of the surface of $CaCO_3$ and NR/$CaCO_3$ composite for PMMA modified $CaCO_3$ (1000X)
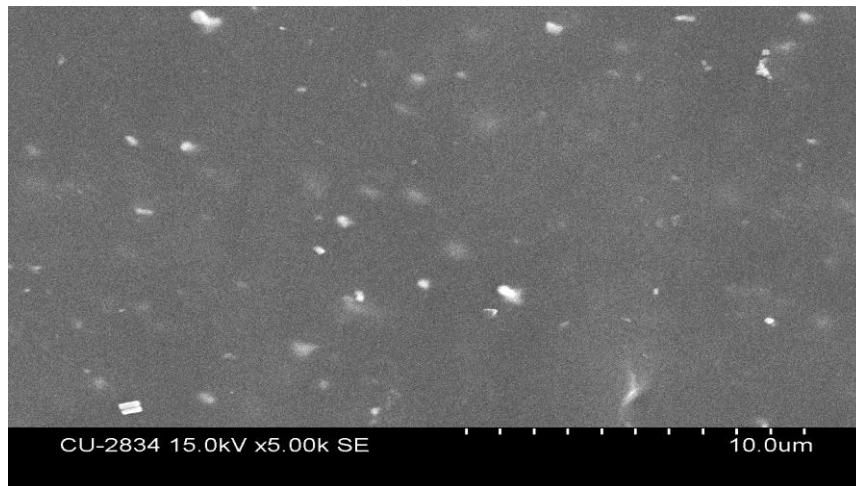
Figure 8c. SEM observation of the surface of $CaCO_3$ and NR/$CaCO_3$ composite for gum compound(S_0) (5000X)
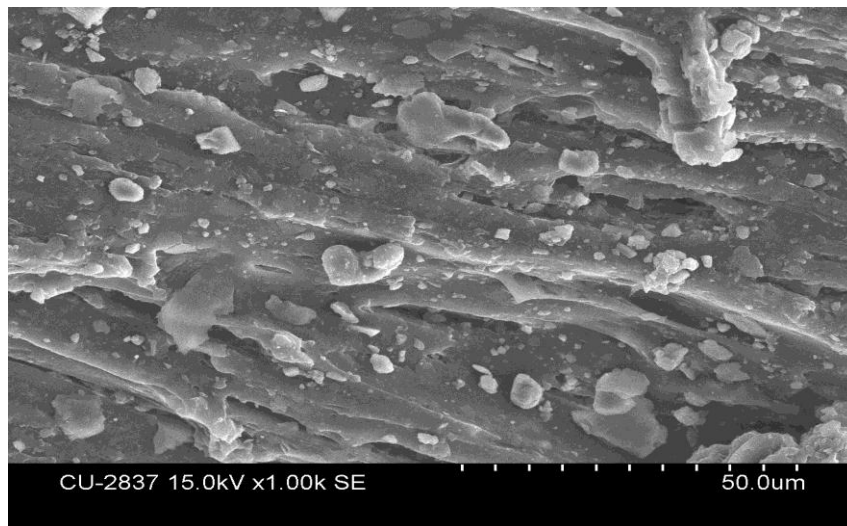
Figure 8d. SEM observation of the surface of $CaCO_3$ and NR/$CaCO_3$ composite for 20 phr $CaCO_3$/NR composite (S_1) (1000X)
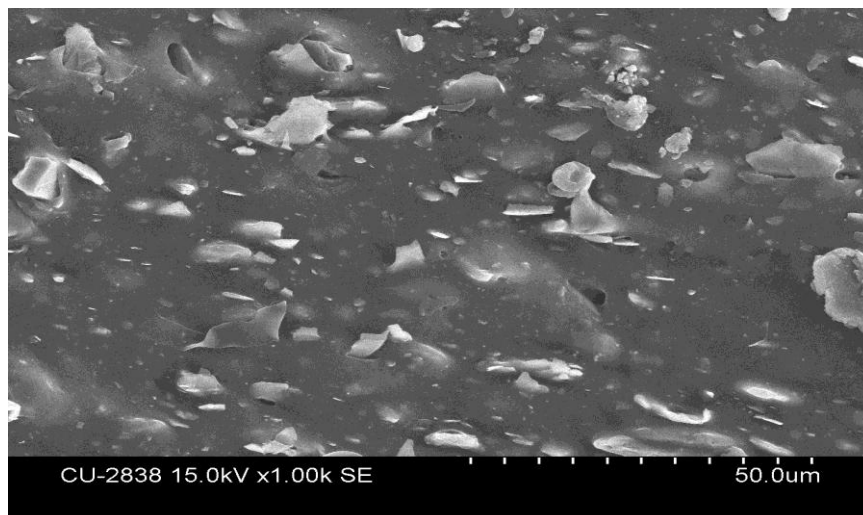
Figure 8e SEM observation of the surface of $CaCO_3$ and NR/$CaCO_3$ composite for 40 phr $CaCO_3$/NR composite (S_2) (1000X)
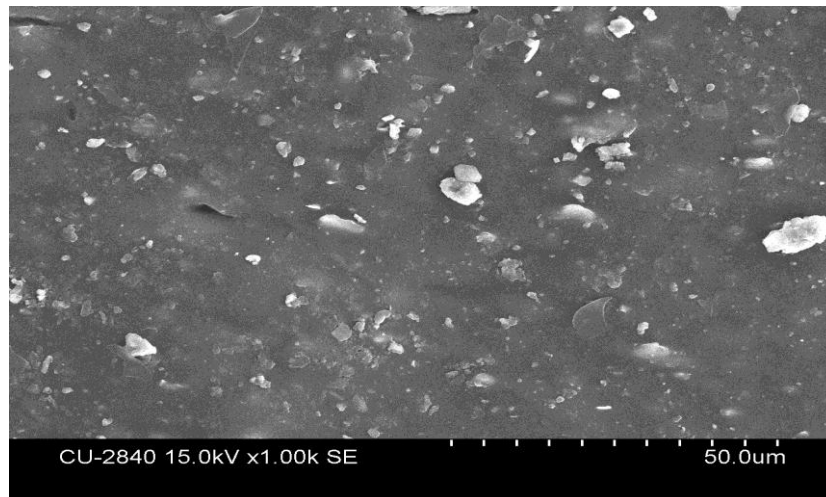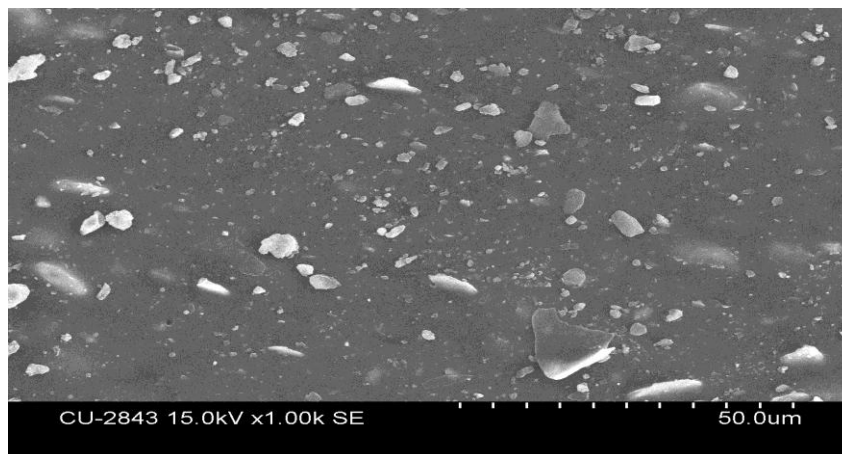

Figure 8f. SEM observation of the surface of CaCO$_3$ and NR/CaCO$_3$ composite for 10 phr modified CaCO$_3$/NR composite (S$_3$) (1000X)

Figure 8g. SEM observation of the surface of CaCO$_3$ and NR/CaCO$_3$ composite for 15 phr modified CaCO$_3$/NR composite (S$_4$) (1000X)
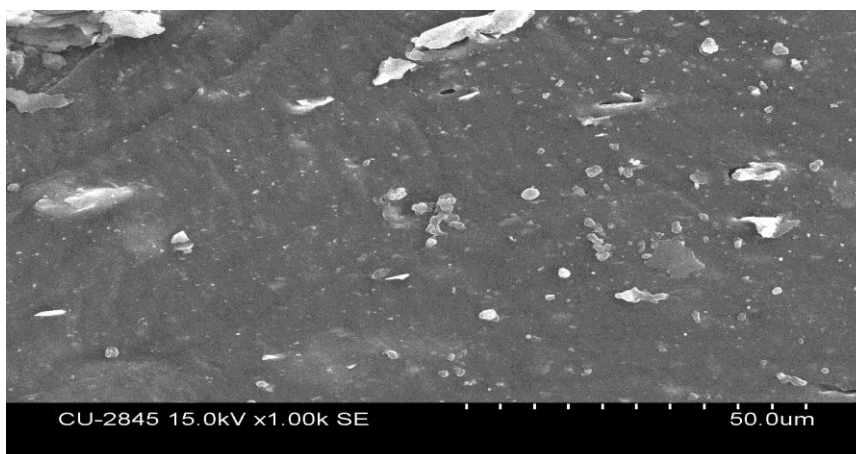

Figure 8h. SEM observation of the surface of CaCO$_3$ and NR/CaCO$_3$ composite for 20 phr modified CaCO$_3$/NR composite (S$_5$) (1000X)